Title

Association of 3D Geometric Measures Derived From Quantitative Computed Tomography With Hip Fracture Risk in Older Men

Journal

Journal of Bone and Mineral Research, 31(8)

ISSN

0884-0431

Authors

Borggrefe, Jan
de Buhr, Timm
Shrestha, Smriti
et al.

Publication Date

2016-08-01

DOI

10.1002/jbmr.2821

Peer reviewed

Published in final edited form as:

J Bone Miner Res. 2016 August ; 31(8): 1550–1558. doi:10.1002/jbmr.2821.

Association of 3-D Geometric Measures derived from Quantitative Computed Tomography with Hip Fracture Risk in Older Men

J. Borggrefe[1,2], **T. de Buhr**[1], **S. Shrestha**[3], **L.M. Marshall**[3,4], **E. Orwoll**[3], **K. Peters**[5], **D. M. Black**[6], **C.-C. Glüer**[1], **Osteoporotic Fractures in Men (MrOS) Study Research Group.**

[1]Sektion Biomedizinische Bildgebung, Klinik für Radiologie und Neuroradiologie, Universitätsklinikum Schleswig-Holstein, Campus Kiel, Germany

[2]Institut und Poliklinik für Diagnostische Radiologie, Uniklinik Köln, Germany

[3]Bone and Mineral Unit, Oregon Health & Science University, Portland, Oregon, USA

[4]Department of Orthopaedics and Rehabilitation, Oregon Health & Science University, Portland, Oregon, USA

[5]California Pacific Medical Center Research Institute, San Francisco.

[6]Department of Epidemiology and Biostatistics, University of California, San Francisco, California, USA

Abstract

We investigated the associations of 3-D geometric measures and volumetric BMD (vBMD) of the proximal femur assessed by quantitative computed tomography (QCT) with hip fracture risk among elderly men.

Prospective case-cohort design nested within the Osteoporotic Fractures in Men Study (MrOS) cohort. QCT scans of 230 men (65 with confirmed hip fractures) were evaluated with Mindways' QCTPRO-BIT software. Measures that are indicative of bone strength for the femoral neck (FN) and for the trochanteric region (TR) were defined. Bending strength measures were estimated by minimum section modulus, buckling strength by buckling ratio and a local thinning index (LTI). Integral and trabecular vBMD measures were also derived. Areal BMD (aBMD) of the total proximal femur from DXA is presented for comparison. Associations of skeletal measures with incident hip fracture were estimated with hazard ratios (HR) per standard deviation and their 95% confidence intervals (CI) from Cox proportional hazard regression models with adjustment for age, BMI, site and aBMD.

Men with hip fractures were older than men without fracture (77.1±6.0 years vs. 73.3±5.7 years, $p<0.01$). Age, BMI and site adjusted HRs were significant for all measures except TR_LTI. Total femural BMD by DXA (HR=4.9, 95%CI: 2.5,9.9), and QCT (HR=5.5, 95%CI: 2.5,11.7), showed the strongest association followed by QCT FN integral vBMD (HR=3.6, 95%CI:1.8,6.9). In models that additionally included aBMD, FN buckling ratio (HR=1.9, 95%CI:1.1,3.2) and

Corresponding Author: Jan Borggrefe, Street Address Department of Diagnostic Radiology, Michaelisstr. 9, D-24105 Kiel, Germany, Phone: ++49 431 597-3156, Fax: ++49 431 597-3127, jan.borggrefe@rad.uni-kiel.de.

trabecular vBMD of the TR (HR=2.0, 95%CI:1.2,3.4) remained associated with hip fracture risk, independent of aBMD.

QCT derived 3-D geometric indices of instability of the proximal femur were significantly associated with incident hip fractures, independent of DXA aBMD. Buckling of the FN is a relevant failure mode not entirely captured by DXA. Further research to study these relationships in women is warranted.

Keywords

Osteoporosis; men; hip fracture; QCT; fracture risk; volumetric bone fragility analysis

Introduction

Improved prediction of hip fracture risk and better understanding of relevant failure modes remain two key goals for the diagnosis and treatment of osteoporosis. The three hip fracture failure modes are; a) insufficiency towards bending forces, b) insufficiency towards torsional forces and c) local buckling failure in the case of excessive cortical thinning. Areal BMD (aBMD) as measured with Dual-X-ray absorptiometry (DXA) is a strong indicator for femoral strength as shown in cadaver studies as well as for clinical hip fracture risk (1–6). Still, the majority of hip fractures occur in subjects in whom hip aBMD is not severely reduced (6,7). Quantitative computed tomography (QCT) can be used to identify and measure geometric features of the proximal femur in three dimensions that have potential to be related to bone strength (8).

The MrOS study group has used femoral QCT to measure femur morphology, volumetric bone mineral density (BMD), bone strength estimated by finite element (FE) analysis and to detect the surrounding soft tissue (9–14). Smaller cross-sectional area, smaller cortical volume, lower trabecular vBMD, and low load-to-strength ratio of the proximal femur all were associated with increased hip fracture risk (9,12) independent of aBMD. However, measures that characterize the strength of specific subregions of bone compartments, such as bending, buckling and torsion, are critical for fragility in regard to relevant failure modes. Only the polar moment of inertia as a cross sectional QCT strength indicator has been examined in relation to fracture risk (13). To date assessment of bending and buckling have been limited to two-dimensional assessments derived from DXA. For example, hip structure analysis (HSA) (15–18), has shown that the defined buckling and bending strength indicators contribute to fracture risk assessment (18).

In comparison to HSA, the 3D QCT assessment of femoral geometry allows to investigate femoral strength indicators in more depth, with the option of determining cortical structure in quadrants of the femoral neck (FN) and the trochanteric region (TR). Thus QCT allows the detection of enhanced focal cortical thinning of the bone cross section which is of considerable interest because it may directly influence buckling and bending strength (18–20). In this study we defined a buckling strength measure derived from QCT data to detect local cortical thinning of quadrants of the femural cross section at the TR and FN, the local thinning index, and tested its performance along with other QCT based structural and

densitometry measures of fragility. The investigation includes measures of severe cortical thinning in subcompartments of the femoral neck (FN) and the trochanteric region (TR), reflecting indicators of strength in the buckling and the bending mode.

We examined the association between these QCT measures of femoral structure and incident hip fracture in a population of older men from the MrOS cohort (21). We also tested whether these associations are independent of other factors associated with fracture, including aBMD as measured by DXA, age, and body mass index (BMI).

Materials and Methods

Subjects

The MrOS Study enrolled 5994 participants from March 2000 through April 2002 as has been previously described (10,21,22). The recruitment occurred at six U.S. academic medical centers in Birmingham AL, Minneapolis MN, Palo Alto CA, Pittsburgh PA, Portland OR, and San Diego CA. Eligible participants were at least 65 years of age, able to walk without assistance from another person, and had not had bilateral hip replacement surgery. All men enrolled in the MrOS cohort provided written informed consent, completed the baseline self-administered questionnaire, and attended the baseline visit at their local site at which skeletal, anthropometric, and other measures were obtained. As described in the earlier MROS publications, the first 650 participants enrolled at each site, and all men from minority backgrounds were referred for QCT scans of the hip and lumbar spine (8, 11). 3786 men referred, 1 refused, and 122 were ineligible for a hip scan because of hip replacement. Ultimately, hip QCT scans of 3663 participants were acquired (61% of the MrOS cohort). Details regarding acquisition of the baseline QCT scans have been described (9). Briefly, the pelvic region was scanned from just above the femoral head to 3.5 cm below the lesser trochanter. The settings of the scanner were 80 kVp, 280 mAs, 3-mm slice thickness, and 512 × 512 matrix with the use of the spiral reconstruction mode. The effective radiation dose associated with this protocol was on the order of 1 mSv or less. A calibration phantom (Image Analysis, Columbia, KY, USA) containing known hydroxyapatite concentrations was included with the participant in every scan. Of the 3663 hip scans, 102 (2.8%) were lost or corrupted during transfer to the central processing site, leaving 3561 available for analysis. Men with a history of hip replacement were ineligible for hip scans. We used a case-cohort sampling design nested within the MrOS study. The randomly selected cohort has already been shown to have similar baseline characteristics as the main MROS cohort (12). In this study QCT scans of 310 men were evaluated (age 74.3 ± 6 years; 90 fracture cases). A thorough data quality check of the QCT scans was performed (see below). Scans for 80 men were excluded from this analysis because their quality was insufficient for the bone segmentation algorithms required of our image processing. 59 patients were excluded due to beam hardening artifacts and consecutive failure in bone segmentation and hip axis definition. Scans for the 230 remaining men included 65 hip fracture cases.

QCT assessment

All QCT scans were obtained at baseline in MrOS (10,11) using a standardized protocol that specified scanning the pelvic region from the femoral head to 3.5 cm below the lesser

trochanter at settings of 80 kVp, 280 mA, 3-mm slice thickness, and 512 × 512 matrix in spiral reconstruction mode. Scanner models used at the sites were GE ProSpeed (Birmingham), GE HiSpeed Advantage (Minneapolis), Phillips MX-8000 (Palo Alto), Siemens Somatom Plus 4 (Pittsburgh), Phillips CT-Twin and Toshiba Acquilion (Portland), and Picker PQ-5000 (San Diego). Calibration standards with known hydroxyapatite concentrations (0 mg/cm^3, 75 mg/cm^3, 150 mg/cm^3; *Image Analysis*®) placed underneath the men were used in each scan for calibration of the scan.

Measurement of quadrants of the femoral cross section and estimation of their structural instability and strength was made using the QCT Pro Bone Investigational Toolkit (BIT, Mindways, Austin Texas) based on a modified version of Mindways' "CTXA Hip Exam Analysis" protocol. Each measure is described in detail below. Men were considered to be eligible if DXA and QCT images were free of artifacts and met all criteria for a valid density calibration as defined by the Mindways software. The skeletal assessments were performed without operator knowledge of hip fracture status.

Femoral neck VOI

The femoral neck axis was located automatically via the "optimize FN axis" option of the BIT software. Along this axis the mid femoral neck volume and the proximal trochanteric volume were defined (Figure 1). The FN Volume of Interest (VOI) of 1.5 cm width was placed manually flanking the trochanter major (comparable with DXA femoral neck box placement on Hologic devices). 11 slices of 1mm thickness each were analyzed. Optimal threshold levels for bone segmentation were identified in a subset of 20 men from the MROS study population. In the visual control of the cortical bone surface of this subgroup at different threshold levels, the cortex threshold of 300 mg/cc was found to be optimal at the femoral neck and a cortex threshold of 250 mg/cc at the trochanteric area. These thresholds allowed accurate automatic cortical segmentation, almost completely avoiding gaps in the segmented cortex even in regions of severe cortical thinning (gaps had no more than one voxel missing). QCT-BIT measurements were performed fully automatically based on a script that was designed for this study.

Trochanteric VOI

In order to identify the level of lowest strength for the trochanteric region we had to evaluate two different trochanteric subregions: (i) for buckling ratio the cross section angulated to be in plane with the intertrochanteric line and the femoral neck was the largest, thus also showing the highest results for buckling ratio; (ii) for the section modulus the plane that comes close to be perpendicular to the femoral shaft is the plane with the smallest cross section and thus in this plane bending strength (Z) is minimal.

Thus, for measures at the TR, a first VOI of 1.0 cm width was manually placed at the maximum cross sectional area of the TR, approximately 1 mm distal of the intertrochanteric line along the axis defined for FN measures (figure 1). A second VOI of the same width was aligned manually along a line bisecting the femoral axis and the axis of the diaphysis in order to detect TR regions with lowest values of bending strength indicators. It was anchored

next to the endosteal surface of the linea terminalis at the distal TR. QCT-BIT measurements again were performed automatically based on a script that was designed for this study.

BMD and 3-D geometric measures:

DXA total hip and femoral neck aBMD measures of the proximal femur and integral QCT vBMD measures of the entire proximal femur were provided from earlier datasets (9). These had all been performed with the same DXA models (4500 W, Hologic, Waltham, MA, USA. All vBMD and structure measures from the FN and TR region were derived from Mindways QCT measurements using the QCTPRO Bone Investigation Toolkit BIT software (Mindways, Austin, Texas).

The section modulus (Z) has been shown to be a relevant structural measure for bending strength as is the buckling ratio (BR) a measure for strength against forces leading to buckling (23). Z is inversely related to stresses exerted by maximum bending loads. QCT as a 3-D measurement allows the evaluation of Z along the strongest (Zmax) and weakest axis (Zmin). When Zmax and Zmin are both considered, they reflect measures related to strength in torsion of the structure. Z is defined as Z=CSMI/r where CSMI (Cross Sectional Moment of Inertia) measures the mass distribution relative to the geometric center (calculated by the Mindways software) and r is the maximal distance from the geometric centre to the periosteal surface for Zmax, or the corresponding periosteal distance in the respective orthogonal direction for Zmin. BR is a measure of cortical instability as a result of excessive cortical thinning. BR relates the cortical thickness to the width of the femoral neck and is defined as $BR=r/ct$, where r is the radius and ct the corresponding cortical thickness. The bone is considered to be vulnerable to the failure mode of buckling when this ratio exceeds 10:1, i.e. BR >10 (24). The results of the 11 slices at the TR and FN were averaged for the data evaluation.

For quadrant analysis of buckling ratio at the weakest FN and TR regions, the cross section was subdivided into 16 sections. This permitted the definition and analysis of quadrants comprised of four adjacent sections each. The BR of the quadrant with the highest focal BR (i.e. r/ct of a quadrant) was defined as local thinning index. All 3D-geometric measures were defined prior to the analysis of the image data.

The image quality assurance, prior to any attempt of analysis, detected failure of cortical bone segmentation in QCTpro software. Here, cases were excluded if inappropriate delineation in the depiction of the segmented cortical bone was seen in the direct comparison of the CT data. Inappropriate delineation of the cortical bone surface was defined as the detection of soft tissue as cortical bone in bone segmentation which could be clearly separated from bone (see supplementary image files Fig. S1–4). As the failure of appropriate bone segmentation and geometric analysis could be associated to operator failure due to inadequate rotation or definition of the soft tissue threshold, we analyzed critical datasets a second time. In the case of persistence of the segmentation error the exclusion criteria were a) based on the visual analysis of the QCTpro BIT analysis sheet which shows how the automatic setting of measurement points for the structural and densitometric data for each reformatted slice was set and b) based on a statistical distribution of the results for all primary outcome variables. If only single slices showed artifacts, these were listed and

excluded from statistical analysis. In the statistical outlier analysis all data were reanalyzed if they fell outside of the 95% confidence interval. If errors could be detected the dataset was excluded from the analysis, else these were kept in the dataset. The primary reason for all data exclusions were beam hardening artifacts (n=59), associated to the low application dose, anatomy and patient positioning. In 9 cases the software reported problems in the bone structural analysis without detectable image problems, most likely due to the phantom calibration. Due to the slow acquisition of the scanners used, 8 subjects showed movement artefacts that prohibited cross sectional image analysis with BIT. In 3 subjects the scan range was to short, which led to a misplacement of the FN axis. 1 patient was excluded due to severe sclerotic changes of the proximal femora. JMP 9.0.1 Software (SAS Institute Inc., Cary, NC, USA) was used for testing the analysis technique on 20 men as well as for the outlier analysis.

Statistical Analysis

Hazard ratios (HR) and 95% confidence intervals (CI) per standard deviation of the BMD or QCT strength indicators were estimated with Cox proportional hazards models. Prentice weights were used to account for the case-cohort sampling design (25). Multivariate models were adjusted for age, BMI and study enrollment site (to account for scanner variation). Further DXA aBMD adjusted models were provided. Harrells C statistics was used to evaluate risk prediction models for hip fracture (26).

Results:

With a mean age of 73.3 ± 5.7 years, the subcohort sample was comparable in age to the main MrOS cohort of the 5994 men (73.7 ± 5.9 years) (9). At baseline, the men who subsequently experienced hip fractures were older than men who remained fracture free (77.1 ± 6.0 years vs. 73.3 ± 5.7 years, $p<0.01$, Table 1). All 3D- geometric measures and densitometric data showed significantly smaller baseline values on average in men who went on to have a hip fracture compared to men who did not experience hip fracture during follow up. We did not note significant differences of baseline parameters between patients who were and were not excluded from the analysis.

Table 2 shows correlations of the 3D- geometric measures with anthropometric and densitometric data. For the femoral neck (Table 2a) bending measures correlated most strongly with DXA aBMD results, whereas buckling ratio correlated best with the QCT-based vBMD. For the trochanter (Table 2b) bending measures again correlated most strongly with DXA aBMD results while weaker correlations were observed for buckling ratio versus aBMD or vBMD results. For both the femoral and the trochanteric area, the measures of bending, but less so for buckling, were associated with height or weight. Both, bending and buckling measures showed the expected age related decline in strength indicators at the femoral neck and the trochanter. LTI showed correlations very similar to buckling ratio (data not shown).

Table 3 lists hazard ratios for all variables evaluated. After adjusting for age, BMI and site, all variables remained significant except TR LTI. DXA aBMD and QCT vBMD of the proximal femur provided the highest hazard ratios overall (HR=4.9, 95% CI: 2.5,9.9 and

HR=5.4, 95% CI: 2.5,11.7). Among single QCT measures of the FN and TR, FN vBMD was the single predictor with the highest HR. Among the strength related measures at the FN, BR provided the highest HR, with slightly lower HRs for Zmin and LTI. In a sensitivity analysis the a priori defined LTI of the superolateral cortex was superior to local thinning indices derived for other quadrants at the FN and TR. At the trochanteric region, trabecular vBMD appeared to be the strongest predictor. Among the strength related measures, Zmin appeared to be strongest here. After additional adjustment for FN aBMD, FN BR (HR=1.9, 95% CI: 1.1,3.2) remained an independent predictor. TR trabecular vBMD (HR=2.0, 95% CI: 1.2,3.4) also contributed independently of aBMD. Replacement of the adjustment for aBMD with vBMD showed comparable results for the structural parameters.

Table 4 shows Harrells C statistics used in order to compare the hip fracture association of QCT measures to DXA. The single parameters with the highest Harrells C values of 0.81 each, adjusted for age, site and BMI, were DXA aBMD and QCT vBMD of the proximal femur. The structural QCT variables BR and FN Zmin of the FN provided an area under the curve of up to 0.79. The highest Harrells C in a multivariate model combing QCT measures with BMD showed Harrells C statistic of 0.82 for DXA aBMD and FN BR or QCT vBMD with FN BR and FN Zmin.

Discussion:

In this study we investigated the associations of QCT measures indicative for geometrical bone instability and strength in key locations of the proximal femur as well as trabecular and cortical volumetric BMD (vBMD) of the proximal femur assessed by quantitative computed tomography (QCT) with hip fracture risk among elderly men. All measures were individually associated with fractures, but, although we did not test for significance of the differences, none were as strongly associated as was aBMD of the proximal femur measured by DXA or QCT. This may not be surprising, since each measure reflects a specific fragility characteristic relevant specific failure mode which may be relevant only for a fraction of fracture cases. BMD on the other hand can be interpreted as a summation measure of fragility relevant for a broader range of impacting loads and therefore it is a more robust overall measure of fragility. Indeed, the observation that some of the strength related measures were associated with fractures independent of BMD suggests that the specific failure modes they reflect have independent predictive value.

As reported in earlier QCT studies for men and women (27), the indicator for bending failure (Zmin) was correlated with aBMD. Despite a similar correlation with aBMD, BR showed an association with fracture risk independent of aBMD, indicating that this index captures fragility aspects that may be related to the relevant failure mode of buckling not entirely reflected in aBMD. Comparable to earlier DXA hip strength analyses (18), BR turned out to be the strongest structural parameter with regard to predictive value at the FN, specifically after adjustment for aBMD. However, as buckling ratio comprises the measures of cross sectional area as well as cortical thickness, it appears that the magnitude of fracture association was lower than it has been reported for cortical thickness alone (13).

The trochanteric fracture risk is known to be strongly associated with low bone mass (28,29). Therefore, it was to be expected that the trabecular vBMD would be a strong predictor. Still the best multivariate model of QCT values at the TR additionally included the bending strength indicator (Zmin) whereas the buckling ratio as an index influenced by cortical thickness and cross sectional area, did not contribute independently. In this regard the measure related to local bending strength performed stronger than it has been reported for polar cross sectional moment of inertia by Yang and colleagues, that was not significantly associated with hip fractures (13)

Recent studies that investigated QCT bone density and bone morphology as indicators of fracture risk in women yielded AUC values for hip fracture prediction that were comparable to the results of our study, both for single variables as well as for multivariate models (30,31). As described in those studies in women, we found in men that both cortical and trabecular parameters are associated with hip fracture risk (9). Further, as described by Yang and colleagues for women (32), and also in our study on men, multivariate regression models showed that QCT-derived measures indicative for bone strength are independently associated with hip fracture risk. However, consistent with these previous reports, our QCT-derived measures did not improve prediction of fracture compared to total hip a BMD.

Cortical bone reduction in the superolateral aspect of the femoral neck has been described to be of particular interest in hip fracture risk assessment (2,19,33). Our findings that buckling is of particular relevance in the femoral neck region in men may help to assess the etiology of hip fractures and to permit a more specific evaluation of the effect of treatment. However, unlike in women (19,34), and comparable to the reports by Yang (13), the prevalence of cortical thinning in this population of men was low (average BR 6.4). In earlier investigations, focal thinning of the superolateral cortex of the femoral neck was hypothesized to be strongly associated with osteoporotic fractures in elderly women (19,20). Despite the association of LTI with fracture risk, these local effects could not be confirmed to be statistically significant in this cohort of men and global cortical thickness of the cross section measured by BR proved to be a stronger predictor than the LTI. Still, in an exploratory sensitivity analysis, our a priori defined LTI of the superolateral cortex was superior to local thinning indices derived for other quadrants at the FN and TR. This may indicate that the superolateral part of the cortex indeed is relevant in terms of fragility. Therefore it would be of particular interest to compare performance of local thinning indices with regard to fracture prediction in women and in men with severe osteoporosis in order to investigate, if buckling failure is a gender issue. Further, subcompartment specific QCT structural analyses may be very useful in studying differences between femur morphology of men suffering cervical fractures compared to those suffering trochanteric fractures. Structural differences relevant for these two fracture types are well established (28,29,35,36) and validation of failure mode specific diagnostic tools, such as QCT structural analysis, may improve risk and therapy assessment.

QCT investigations of bone geometry have strengths and limitations. In terms of strengths, most importantly, they allow testing of whether a specific quadrant or a specific failure mode is of particular relevance for hip fracture risk. Discrete local changes induced by drug therapy can be tested as to what extent they reduce the risks of buckling at the femoral neck

or bending at the trochanter. The method tested in this study and the measures derived can be used in such an assessment. In terms of limitations, an index tailored to be particularly sensitive to a specific failure type may be less optimal to reflect overall hip fracture risk under a variety of unpredictable loading conditions. Indeed, we observed that BMD as an integrated index showed substantially stronger predictive power when used as a single risk index. Unlike QCT vBMD, which is independent of bone geometry, DXA aBMD increases with increased bone size, as does bone strength, and thus one could argue that this size dependency may strengthen its predictive power. However, at least for total femur measurements, our data do not support this argument, since QCT vBMD total hip performs at least as good as DXA aBMD total hip. The disadvantage of more specific strength measures may be overcome by combinations of several (of our) strength related measures, as suggested by the results of our multivariate models. In summary, QCT-derived estimates of bone strength examined here were less strongly associated with fracture risk than BMD. However, the QCT based measures of BR were independently associated with hip fracture risk after adjustment for BMD, suggesting they captured unique information about fracture. Although the increase of AUC was negligible just as it has been reported for vBMD measurements of the entire study population (8), these findings should be verified in additional populations.

In their latest position development conference, the ISCD recommends not to use buckling ratio (and other geometric measures) assessed by DXA for hip fracture risk assessment or treatment indications (37,38).Our study does not contradict the ISCD position statement. These statements are designed to guide clinicians and those may be misled in their assessment of a patient’s risk status by being able to choose from many potential predictors of risk. When picking the variable indicating the highest risk, a large number of false positive risk estimates may be expected simply due to chance. The ISCD guidance is very helpful here to point the doctor to the most robust variable(s). Our study, however, serves an entirely different purpose: we would like to unravel the factors that contribute to bone structural fragility. It is conceivable that there are multiple contributing factors and only once these have been established they can potentially be combined into a single measure of risk. In this paper we mostly work on the identification stage and in this setting we had to investigate multiple variables. Our multivariate models give first indications how these multiple potential predictors differ and whether any of them contributes complementing information. BR showed contributions to fracture risk independent of aBMD which may indicate some relevance of buckling as a failure mode in osteoporotic fractures. Still, at this stage inclusion of BR did not significantly increase overall predictive power. Whether BR may have a role in the context of QCT based assessments requires further study. In this context it remains to be tested whether BR remains predictive after adjustment for cortical thickness or volume which were not measured in this study.

Despite its strong performance in hip fracture risk prediction, DXA also has intrinsic limitations. For example, many patients with hip fracture do not have markedly low levels of aBMD (6,39). As an alternative method in the detection of bone strength associated measures, QCT provides insight into bone geometry and more specific data about bone density in the cortical and trabecular compartments. The potential to analyze quadrants of the bone cross section may point to different areas of focal fragility, which may improve

personalized risk assessment for some patients (20) and it may also help to assess treatment effects in more detail (23). However, one has to note that QCT fails to improve risk prediction compared to DXA. The limited correlation of DXA and QCT results (e.g. table 2b) indicates that these techniques will in part identify different patients to be at high risk with none of the techniques offering superior overall predictive power.

Our study has some limitations. In general, QCT segmentation of the cortex may fail in cases of suboptimal resolution or artifacts. Accuracy and precision of the measurements might be effected significantly by the segmentation thresholds and the VOI definition. Especially in the TR, the axis for the positioning of the VOI is less evident than at the FN and thus might be defined with a lower precision. For the adapted QCT protocols we used CT-scanners with suboptimal performance compared to today's technological standards. Therefore, the presence of artifacts resulted in a high rate of exclusions from analysis (~26%) and the segmented cortical bone included subcortical bone tissue due to partial volume effects. Thus, the evaluation of several of our 3-D geometric measures, most importantly local thinning, was hampered by partial volume effects and could likely be improved by better image resolution (40) which would be at the expense of higher radiation exposure (41). Furthermore, the CT data acquisition with 80 kVp led to a considerable image noise in many cases, resulting in a higher variability of CT measures. The trochanteric and cervical fractures were analyzed jointly although intracapsular and trochanteric fractures are considered to have different pathophysiology (42). Thus it may be worth while identifying predictors of strength specific to these different types of fractures. Once identified, one could recombine fracture type specific risk into an overall risk of hip fracture. Improved image processing for better delineation of the cortex (43) may also yield improved estimates of the measures proposed and tested here. However, it requires resolution in the micron range to detect further relevant cortical structural impairments such as focal porosity or micro-cracks, which cannot be provided with regular QCT measurements (44). All procedures have their estimation error due to reproducibility of positioning and the measurement procedure which are not provided for our QCT methods. Buckling ratio is an established measure in biomechanics but the subsection index may require further refinement and needs further testing in independent samples. Moreover, soft tissue thickness measures and soft tissue analyses that can be integrated in clinical QCT evaluation may additionally improve the prediction of fracture risk (45).

In conclusion, while areal BMD as assessed by DXA was found to be most highly associated with hip fracture risk in men, we showed that QCT derived 3-D geometric measures as indicators of hip strength remain associated with hip fracture risk after adjustment for BMD. Although combined models of risk were not significantly stronger than those based on age, BMI and site adjusted BMD alone, these QCT-based measurements may permit insight into the biomechanics of fracture. Further research to study these relationships in women is warranted.

Supplementary Material

Refer to Web version on PubMed Central for supplementary material.

Acknowledgements.

We would like to thank Keenan Brown (Mindways Inc.) for providing software enhancements for the QCTPro software designed specifically for this study. The Osteoporotic Fractures in Men (MrOS) Study is supported by National Institutes of Health funding. The following institutes provide support: the National Institute on Aging (NIA), the National Institute of Arthritis and Musculoskeletal and Skin Diseases (NIAMS), the National Center for Advancing Translational Sciences (NCATS), and NIH Roadmap for Medical Research under the following grant numbers: U01 AG027810, U01 AG042124, U01 AG042139, U01 AG042140, U01 AG042143, U01 AG042145, U01 AG042168, U01 AR066160, and UL1 TR000128.

Literature:

1. Gnudi S, Ripamonti C, Gualtieri G, Malavolta N 1999 Geometry of proximal femur in the prediction of hip fracture in osteoporotic women. Br J Radiol 72:729–33. [PubMed: 10624337]
2. Bell KL, Loveridge N, Power J, Rushton N, Reeve J 1999 Intracapsular hip fracture: increased cortical remodeling in the thinned and porous anterior region of the femoral neck. Osteoporos Int 10:248–57. [PubMed: 10525718]
3. Bouxsein ML, Karasik D 2006 Bone geometry and skeletal fragility. Curr Osteoporos Rep 4:49–56. [PubMed: 16822403]
4. Cheng XG, Lowet G, Boonen S, Nicholson PH, Brys P, Nijs J, Dequeker J 1997 Assessment of the strength of proximal femur in vitro: relationship to femoral bone mineral density and femoral geometry. Bone 20:213–8. [PubMed: 9071471]
5. Johnell O, Kanis JA, Oden A, Johansson H, De Laet C, Delmas P, Eisman JA, Fujiwara S, Kroger H, Mellstrom D, Meunier PJ, Melton LJ 3rd, O'Naeill T, Pols H, Reeve J, Silman A, Tenenhouse A 2005 Predictive value of BMD for hip and other fractures. J Bone Miner Res 20:1185–94. [PubMed: 15940371]
6. Siris ES, Chen YT, Abbott TA, Barrett-Connor E, Miller PD, Wehren LE, Berger ML 2004 Bone mineral density thresholds for pharmacological intervention to prevent fractures. Arch Intern Med 164:1108–12. [PubMed: 15159268]
7. Wainwright SA, Marshall LM, Ensrud KE, Cauley JA, Black DM, Hillier TA, Hochberg MC, Vogt MT, Orwoll ES 2005 Hip fracture in women without osteoporosis. J Clin Endocrinol Metab 90:2787–93. [PubMed: 15728213]
8. Danielson ME, Beck TJ, Karlamangla AS, Greendale GA, Atkinson EJ, Lian Y, Khaled AS, Keaveny TM, Kopperdahl D, Ruppert K, Greenspan S, Vuga M, Cauley JA 2012 A comparison of DXA and CT based methods for estimating the strength of the femoral neck in post-menopausal women. Osteoporos Int 24:1379–88. [PubMed: 22810918]
9. Black DM, Bouxsein ML, Marshall LM, Cummings SR, Lang TF, Cauley JA, Ensrud KE, Nielson CM, Orwoll ES 2008 Proximal femoral structure and the prediction of hip fracture in men: a large prospective study using QCT. J Bone Miner Res 23:1326–33. [PubMed: 18348697]
10. Marshall LM, Lang TF, Lambert LC, Zmuda JM, Ensrud KE, Orwoll ES 2006 Dimensions and volumetric BMD of the proximal femur and their relation to age among older U.S. men. J Bone Miner Res 21:1197–206. [PubMed: 16869717]
11. Marshall LM, Zmuda JM, Chan BK, Barrett-Connor E, Cauley JA, Ensrud KE, Lang TF, Orwoll ES 2008 Race and ethnic variation in proximal femur structure and BMD among older men. J Bone Miner Res 23:121–30. [PubMed: 17892375]
12. Orwoll ES, Marshall LM, Nielson CM, Cummings SR, Lapidus J, Cauley JA, Ensrud K, Lane N, Hoffmann PR, Kopperdahl DL, Keaveny TM 2009 Finite element analysis of the proximal femur and hip fracture risk in older men. J Bone Miner Res 24:475–83. [PubMed: 19049327]
13. Yang L, Burton AC, Bradburn M, Nielson CM, Orwoll ES, Eastell R 2012 Distribution of bone density in the proximal femur and its association with hip fracture risk in older men: the osteoporotic fractures in men (MrOS) study. J Bone Miner Res 27:2314–24. [PubMed: 22729872]
14. Nielson CM, Bouxsein ML, Freitas SS, Ensrud KE, Orwoll ES 2009 Trochanteric soft tissue thickness and hip fracture in older men. J Clin Endocrinol Metab 94:491–6. [PubMed: 19017753]
15. Beck TJ, Looker AC, Ruff CB, Sievanen H, Wahner HW 2000 Structural trends in the aging femoral neck and proximal shaft: analysis of the Third National Health and Nutrition Examination

Survey dual-energy X-ray absorptiometry data. J Bone Miner Res 15:2297–304. [PubMed: 11127194]

16. Beck TJ, Oreskovic TL, Stone KL, Ruff CB, Ensrud K, Nevitt MC, Genant HK, Cummings SR 2001 Structural adaptation to changing skeletal load in the progression toward hip fragility: the study of osteoporotic fractures. J Bone Miner Res 16:1108–19. [PubMed: 11393788]
17. Beck TJ, Ruff CB, Warden KE, Scott WW Jr., Rao GU 1990 Predicting femoral neck strength from bone mineral data. A structural approach. Invest Radiol 25:6–18. [PubMed: 2298552]
18. Kaptoge S, Beck TJ, Reeve J, Stone KL, Hillier TA, Cauley JA, Cummings SR 2008 Prediction of incident hip fracture risk by femur geometry variables measured by hip structural analysis in the study of osteoporotic fractures. J Bone Miner Res 23:1892–904. [PubMed: 18684092]
19. Mayhew PM, Thomas CD, Clement JG, Loveridge N, Beck TJ, Bonfield W, Burgoyne CJ, Reeve J 2005 Relation between age, femoral neck cortical stability, and hip fracture risk. Lancet 366:129–35. [PubMed: 16005335]
20. Poole KE, Mayhew PM, Rose CM, Brown JK, Bearcroft PJ, Loveridge N, Reeve J 2009 Changing Structure of the Femoral Neck Across the Adult Female Lifespan. J Bone Miner Res.
21. Orwoll E, Blank JB, Barrett-Connor E, Cauley J, Cummings S, Ensrud K, Lewis C, Cawthon PM, Marcus R, Marshall LM, McGowan J, Phipps K, Sherman S, Stefanick ML, Stone K 2005 Design and baseline characteristics of the osteoporotic fractures in men (MrOS) study--a large observational study of the determinants of fracture in older men. Contemp Clin Trials 26:569–85. [PubMed: 16084776]
22. Blank JB, Cawthon PM, Carrion-Petersen ML, Harper L, Johnson JP, Mitson E, Delay RR 2005 Overview of recruitment for the osteoporotic fractures in men study (MrOS). Contemp Clin Trials 26:557–68. [PubMed: 16085466]
23. Borggrefe J, Graeff C, Nickelsen TN, Marin F, Gluer CC 2010 Quantitative computed tomographic assessment of the effects of 24 months of teriparatide treatment on 3D femoral neck bone distribution, geometry, and bone strength: results from the EUROFORS study. J Bone Miner Res 25:472–81. [PubMed: 19778182]
24. Young W 1989 Elastic stability formulas for stress and strain In: Crawford HTS, editor. Roark's Formulas for Stress and Strain, 6th ed New York' McGraw-Hill:688.
25. Barlow WE, Ichikawa L, Rosner D, Izumi S 1999 Analysis of case-cohort designs. J Clin Epidemiol 52:1165–72. [PubMed: 10580779]
26. Uno H, Cai T, Pencina MJ, D'Agostino RB, Wei LJ 2011 On the C-statistics for evaluating overall adequacy of risk prediction procedures with censored survival data. Stat Med 30:1105–17. [PubMed: 21484848]
27. Ahlborg HG, Nguyen ND, Nguyen TV, Center JR, Eisman JA 2005 Contribution of hip strength indices to hip fracture risk in elderly men and women. J Bone Miner Res 20:1820–7. [PubMed: 16160739]
28. Lang TF, Augat P, Lane NE, Genant HK 1998 Trochanteric hip fracture: strong association with spinal trabecular bone mineral density measured with quantitative CT. Radiology 209:525–30. [PubMed: 9807584]
29. Mautalen CA, Vega EM, Einhorn TA 1996 Are the etiologies of cervical and trochanteric hip fractures different? Bone 18:133S–137S. [PubMed: 8777078]
30. Bousson VD, Adams J, Engelke K, Aout M, Cohen-Solal M, Bergot C, Haguenauer D, Goldberg D, Champion K, Aksouh R, Vicaut E, Laredo JD 2011 In vivo discrimination of hip fracture with quantitative computed tomography: results from the prospective European Femur Fracture Study (EFFECT). J Bone Miner Res 26:881–93. [PubMed: 20939025]
31. Yang L, Udall WJ, McCloskey EV, Eastell R 2013 Distribution of bone density and cortical thickness in the proximal femur and their association with hip fracture in postmenopausal women: a quantitative computed tomography study. Osteoporos Int 25:251–63. [PubMed: 23719860]
32. Yang L, Udall WJ, McCloskey EV, Eastell R 2013 Distribution of bone density and cortical thickness in the proximal femur and their association with hip fracture in postmenopausal women: a quantitative computed tomography study. Osteoporos Int.
33. Crabtree NJ, Kroger H, Martin A, Pols HA, Lorenc R, Nijs J, Stepan JJ, Falch JA, Miazgowski T, Grazio S, Raptou P, Adams J, Collings A, Khaw KT, Rushton N, Lunt M, Dixon AK, Reeve J

2002 Improving risk assessment: hip geometry, bone mineral distribution and bone strength in hip fracture cases and controls. The EPOS study. European Prospective Osteoporosis Study. Osteoporos Int 13:48–54. [PubMed: 11883408]

34. Rivadeneira F, Zillikens MC, De Laet CE, Hofman A, Uitterlinden AG, Beck TJ, Pols HA 2007 Femoral Neck BMD is a Strong Predictor of Hip Fracture Susceptibility in Elderly Men and Women Because it Detects Cortical Bone Instability: The Rotterdam Study. J Bone Miner Res.
35. Carpenter RD, Beaupre GS, Lang TF, Orwoll ES, Carter DR 2005 New QCT analysis approach shows the importance of fall orientation on femoral neck strength. J Bone Miner Res 20:1533–42. [PubMed: 16059625]
36. de Bakker PM, Manske SL, Ebacher V, Oxland TR, Cripton PA, Guy P 2009 During sideways falls proximal femur fractures initiate in the superolateral cortex: evidence from high-speed video of simulated fractures. J Biomech 42:1917–25. [PubMed: 19524929]
37. Engelke K, Lang T, Khosla S, Qin L, Zysset P, Leslie WD, Shepherd JA, Schousboe JT 2015 Clinical Use of Quantitative Computed Tomography (QCT) of the Hip in the Management of Osteoporosis in Adults: the 2015 ISCD Official Positions-Part I. J Clin Densitom 18:338–58. [PubMed: 26277851]
38. Shepherd JA, Schousboe JT, Broy SB, Engelke K, Leslie WD 2015 Executive Summary of the 2015 ISCD Position Development Conference on Advanced Measures From DXA and QCT: Fracture Prediction Beyond BMD. J Clin Densitom 18:274–86. [PubMed: 26277847]
39. Schuit SC, van der Klift M, Weel AE, de Laet CE, Burger H, Seeman E, Hofman A, Uitterlinden AG, van Leeuwen JP, Pols HA 2004 Fracture incidence and association with bone mineral density in elderly men and women: the Rotterdam Study. Bone 34:195–202. [PubMed: 14751578]
40. Hangartner TN, Gilsanz V 1996 Evaluation of cortical bone by computed tomography. J Bone Miner Res 11:1518–25. [PubMed: 8889852]
41. Damilakis J, Adams JE, Guglielmi G, Link TM 2010 Radiation exposure in X-ray-based imaging techniques used in osteoporosis. Eur Radiol 20:2707–14. [PubMed: 20559834]
42. Pulkkinen P, Gluer CC, Jamsa T 2011 Investigation of differences between hip fracture types: a worthy strategy for improved risk assessment and fracture prevention. Bone 49:600–4. [PubMed: 21807130]
43. Treece GM, Gee AH, Mayhew PM, Poole KE 2010 High resolution cortical bone thickness measurement from clinical CT data. Med Image Anal 14:276–90. [PubMed: 20163980]
44. Bell KL, Loveridge N, Power J, Garrahan N, Meggitt BF, Reeve J 1999 Regional differences in cortical porosity in the fractured femoral neck. Bone 24:57–64. [PubMed: 9916785]
45. Bouxsein ML, Szulc P, Munoz F, Thrall E, Sornay-Rendu E, Delmas PD 2007 Contribution of trochanteric soft tissues to fall force estimates, the factor of risk, and prediction of hip fracture risk. J Bone Miner Res 22:825–31. [PubMed: 17352651]

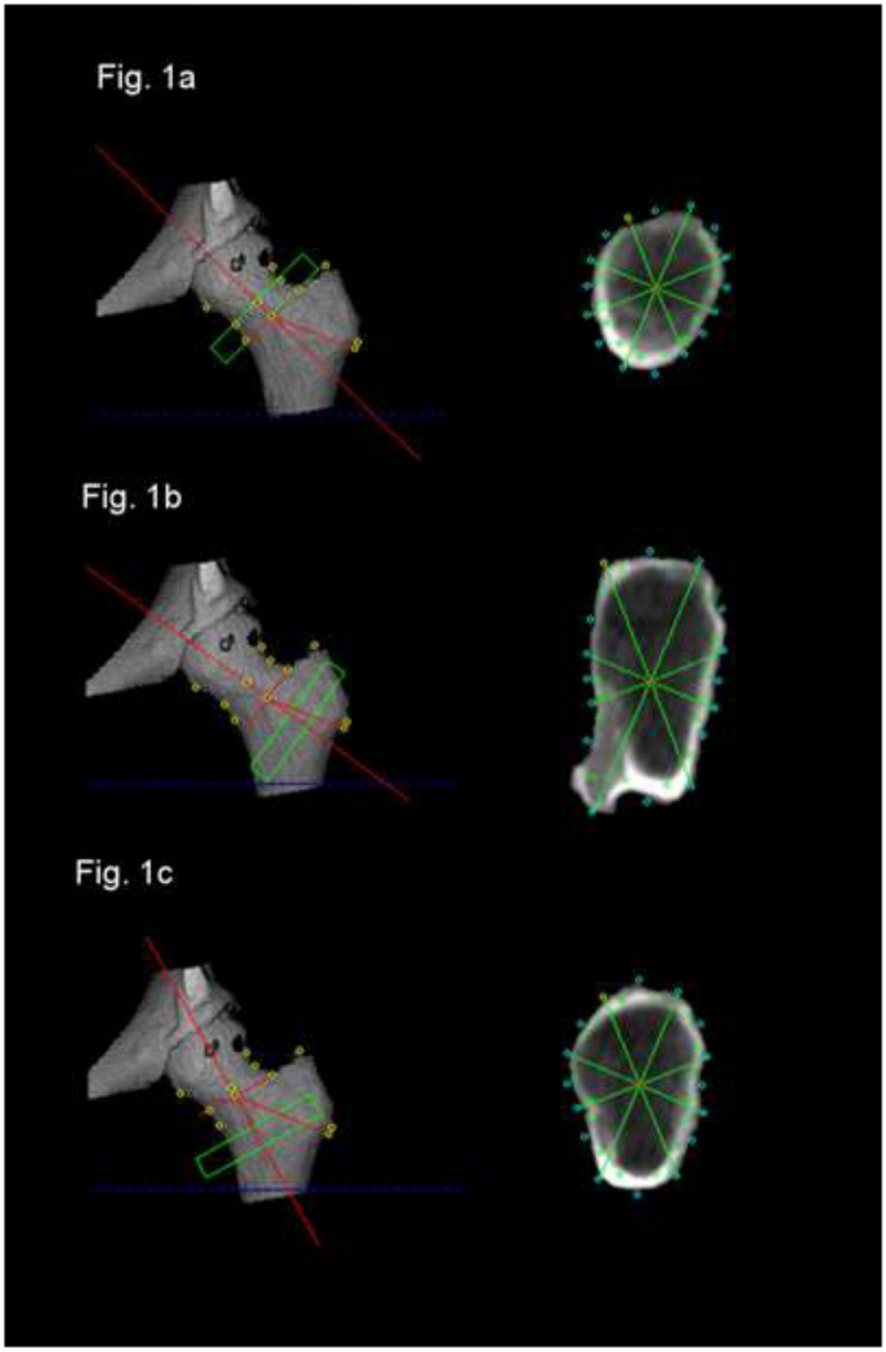

Figure 1:
Definition of the volumes of interest for structural bone analysis at the FN and TR as defined with QCTpro software in the volume depiction of the proximal femur. Corresponding Cross sectional image data used for structural analysis of the FN (Fig.1a), Buckling strength in the TR (Fig.1b) and bending strength as well as densitometry in the TR (Fig. 1c).

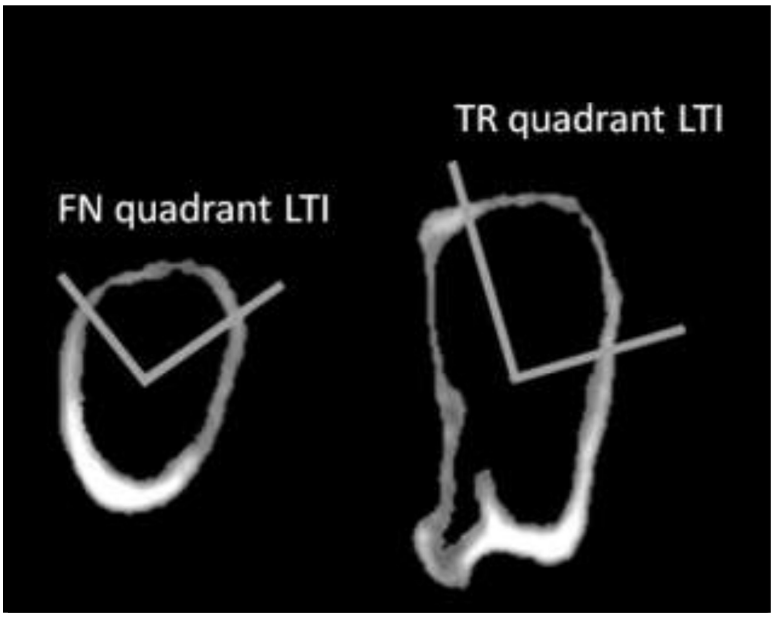

Fig. 2:
Depiction of the cortical bone in the cross sectional slices of the FN and the TR as defined with QCTpro in the process of the image analysis. The upper quadrants of the TR and FN showed the highest LTI in a preceding statistical analysis on 20 men and were used to define the volume of local cortical thinning.

Table 1.

Baseline characteristics of men who remained fracture free (control group) compared to men who experienced a hip fracture during follow up. TH = total hip, FN= femoral neck, TR= trochanteric region, BMI= body mass index, vBMD = volumetric bone mineral density derived by quantitative computed tomography, Zmin= the bending strength index minimal section modulus, LTI = local thinning index.

	No hip fracture N= 165		**Hip fracture cases N= 65**		
	Mean	**SD**	**Mean**	**SD**	**p**
Age [years]	73.3	5.7	77.1	6.0	<0.01
Height [cm]	174.7	7.8	173.8	6.1	0.38
Weight [kg]	83.5	12.9	79.2	12.4	0.02
BMI [kg/m^2]	27.3	3.4	26.2	3.8	0.03
TH BMD integral [g/cm^3]	0.28	0.04	0.23	0.05	<0.01
FN Zmin [cm^3]	1.8	0.42	1.6	0.32	<0.01
FN Buckling Ratio	5.2	1.3	6.8	1.9	<0.01
FN LTI	14.8	5.9	20.2	6.8	<0.01
FN vBMD integral [g/cm^3]	0.29	0.05	0.24	0.05	<0.01
TR Zmin [cm^3]	4.97	0.77	4.52	0.64	<0.01
TR Buckling Ratio	10.4	2.0	11.7	2.4	<0.01
TR LTI	29.4	13.3	35.6	15.2	<0.01
TR vBMD trab. [g/cm^3]	0.11	0.03	0.07	0.04	<0.01

p value for comparison of means

*LTI and BR are unitless

Table 2a.

Spearman Correlations between the various 3-D geometric measures in the femoral neck region and characteristics of men

	Zmin		Buckling ratio		Femoral neck vBMD integral [g/cm^3]	
	(R)	**p**	**(R)**	**p**	**(R)**	**p**
Age [years]	−0.25	<0.01	0.29	<0.01	−0.21	<0.01
Height [cm]	0.38	<0.01	0.12	0.07	−0.04	<0.59
Weight [kg]	0.41	<0.01	−0.12	0.07	0.21	<0.01
BMI	0.24	<0.01	−0.21	<0.01	0.27	<0.01
Femoral neck aBMD	0.58	<0.01	−0.64	<0.01	0.69	<0.01
Total hip aBMD	0.56	<0.01	−0.59	<0.01	0.66	<0.01
Femoral neck vBMD integral [g/cm^3]	0.47	<0.01	−0.79	<0.01		

Table 2b.

Spearman Correlations between the various 3-D geometric measures in the trochanteric region and characteristics of men

	Zmin		Buckling ratio		Femoral neck vBMD integral [g/cm^3]	
	(R)	**p**	**(R)**	**p**	**(R)**	**p**
Age [years]	−0.22	<0.01	0.25	<0.01	−0.21	<0.01
Height [cm]	0.43	<0.01	−0.04	0.59	−0.04	<0.01
Weight [kg]	0.48	<0.01	−0.21	<0.01	0.21	<0.01
BMI	0.28	<0.01	−0.21	<0.01	0.27	<0.01
Femoral neck aBMD	0.53	<0.01	−0.43	<0.01	0.69	<0.01
Total hip aBMD	0.58	<0.01	−0.45	<0.01	0.66	<0.01
Femoral neck vBMD integral [g/cm^3]	0.43	<0.01	−0.42	<0.01		

R, Spearmen correlation coefficient

Table 3.

Hazard Ratios and 95% confidence intervals for incident hip fracture per SD increment in the skeletal measure. The aBMD adjusted models were adjusted for aBMD total.*,**

	Model				
	Unadjusted	**Age, BMI and site adjusted**	**Age, BMI, site and aBMD adjusted**	**Age, BMI, site and vBMD integral adjusted**	**Age, BMI, site and vBMD FN adjusted**
DXA aBMD total [g/cm^2]	5.4 (3.1, 9.5)	4.9 (2.5, 9.9)		2.1 (1.0, 4.7)	3.1 (1.5, 6.5)
FN Zmin [cm^3]	2.3 (1.6, 3.2)	2.0 (1.3, 3.0)	1.0 (0.7, 1.6)	1.3 (0.8, 2.1)	1.5 (1.0, 2.4)
FN Buckling Ratio	3.0 (1.9, 4.5)	2.9 (1.9, 4.6)	1.9 (1.1, 3.2)	1.8 (1.0, 3.0)	1.9 (1.0, 3.7)
FN LTI	2.5 (1.8, 3.5)	2.2 (1.4, 3.2)	1.4 (0.9, 2.3)	1.4 (0.8, 2.3)	1.4 (0.8–2.4)
FN vBMD integral [g/cm^3]	4.0 (2.3, 7.0)	3.6 (1.8, 6.9)	2.0 (1.0, 4.0)	0.7 (0.2, 2.1)	
TR Zmin [cm^3]	2.3 (1.6, 3.3)	2.0 (1.4, 3.0)	0.9 (0.5, 1.6)	1.2 (0.7, 1.9)	1.6 (1.0, 2.5)
TR Buckling Ratio	1.6 (1.2, 2.1)	1.6 (1.1, 2.3)	1.3 (0.8, 2.0)	1.5 (1.0, 2.3)	1.7 (1.2, 2.4)
TR LTI	1.4 (1.1, 1.8)	1.3 (0.9, 1.8)	1.2 (0.8, 1.8)	1.0 (0.7, 1.6)	1.2 (0.8, 1.8)
TR vBMD trab [mg/cm^3]	3.3 (2.0,5,3)	3.2 (1.9,5.4)	2.0 (1.2, 3.4)	1,2 (0.6, 2.5)	1.9 (1.0, 3.7)

95% CIs shown in parentheses

* Fracture risk increased per SD decrease of Z, vBMD, aBMD, and per SD increase in BR as well as LTI n=230 for both femoral neck and trochanteric group

** LTI and BR are unit-less.

Table 4.

Age, BMI and site adjusted models for hip fracture association. Harrels C for the single parameters DXA aBMD and QCT vBMD of the proximal femur. ROC model of 3-D geometric measures at the FN and TR.

	Harrells C	HR (95% CI)
DXA aBMD total hip	0.81	4.9 (2.5, 9.9)
QCT vBMD total hip	0.81	5.4 (2.5, 11.7)
QCT vBMD FN	0.78	3.6 (1.8, 6.9)
FN BR	0.79	2.6 (1.6, 4.1)
+ FN_ZMIN		1.6 (1.1, 2.5)
TR_BR	0.75	1.3 (0.9, 1.9)
+TR_ZMIN		1.7 (1.2, 2.6)
QCT vBMD total hip	0.81	3.8 (1.7, 8.5)
+ FN BR		1.8 (1.1, 3.1)
DXA aBMD total hip	0.82	3.3 (1.6, 6.7)
+ FN BR		1.9 (1.1, 3.2)
QCT vBMD total hip	0.81	5.0 (2.3, 10.7)
+ FN Zmin		1.3 (0.8, 2.1)
DXA aBMD total hip	0.81	4.8 (2.2, 10.5)
+ FN Zmin		1.1 (0.7, 1.6)
QCT vBMD total hip	0.81	5.1 (2.3, 11.2)
+ TR_Zmin		1.2 (0.7, 1.9)
DXA aBMD total hip	0.81	5.3 (2.1, 13.2)
+ TR_Zmin		0.9 (0.5, 1.6)
QCT vBMD total hip	0.81	4.2 (1.9, 9.3)
+ TR vBMD trab		1.4 (0.8, 2.6)
DXA aBMD total hip	0.81	3.8 (1.9, 7.7)
+ TR vBMD trab		2.0 (1.2, 3.4)
QCT vBMD total hip	0.82	3.6 (1.6, 8.0)
+ FN BR		1.7 (1.0, 3.0)
+ FN Zmin		1.3 (0.8, 2.1)
DXA aBMD total hip	0.81	3.1 (1.4, 6.8)
+ FN BR		1.9 (1.1, 3.3)
+ FN Zmin		1.1 (0.7, 1.9)
QCT vBMD total hip	0.81	5.2 (0.9, 2.8)
+ TR BR		1.5 (1.1, 2.4)

	Harrells C	HR (95% CI)
+ TR Zmin		0.9 (0.6, 1.6)
DXA aBMD total hip	0.81	5.0 (2.1, 11.8)
+ TR BR		1.3 (0.8, 2.1)
+ TR Zmin		0.8 (0.5, 1.4)
QCT vBMD total hip	0.82	2.9 (1.2, 6.9)
+ FN BR		1.6 (0.9, 2.8)
+ FN Zmin		1.3 (0.8, 2.2)
+ TR vBMD trab		1.3 (0.7, 2.6)
DXA aBMD total hip	0.81	2.6 (1.1, 5.9)
+ FN BR		1.7 (0.9, 2.9)
+ FN Zmin		1.3 (0.7, 2.2)
+ TR vBMD trab		1.8 (1.0, 3.4)